LECTURE 3: Fluid Statics

We begin by considering static fluid configurations, for which the stress tensor reduces to the form $\mathbf{T} = -p\mathbf{I}$, so that $\mathbf{n} \cdot \mathbf{T} \cdot \mathbf{n} = -p$, and the normal stress balance assumes the form:

$$\hat{p} - p \;=\; \sigma \, \nabla \cdot \mathbf{n} \tag{1}$$

The pressure jump across the interface is balanced by the curvature force at the interface. Now since $\mathbf{n} \cdot \mathbf{T} \cdot \mathbf{s} = 0$ for a static system , the tangential stress balance equation indicates that: $0 = \nabla\sigma$. This leads us to the following important conclusion:

There cannot be a static system in the presence of surface tension gradients. While pressure jumps can sustain normal stress jumps across a fluid interface, they do not contribute to the tangential stress jump. Consequently, tangential surface stresses can only be balanced by viscous stresses associated with fluid motion.

We proceed by applying equation (1) to a number of static situations.

3.1 Stationary bubble

We consider a spherical bubble of radius R submerged in a static fluid. What is the pressure drop across the bubble surface?

The curvature of the spherical surface is simply computed:

$$\nabla \cdot \mathbf{n} \;=\; \nabla \cdot \mathbf{r} \;=\; \frac{1}{r^2}\frac{\partial}{\partial r}(r^2) \;=\; \frac{2}{R} \tag{2}$$

so the normal stress jump (1) indicates that

$$\hat{p} - p \;=\; \frac{2\sigma}{R} \quad . \tag{3}$$

The pressure within the bubble is higher than that outside by an amount proportional to the surface tension, and inversely proportional to the bubble size. It is thus that small bubbles are louder than large ones when they burst at a free surface: champagne is louder than beer. We note that soap bubbles in air have two surfaces that define the inner and outer surfaces of the soap film; consequently, the pressure differential is twice that across a single interface.

3.2 Static meniscus

Consider a situation where the pressure within a static fluid varies owing to the presence of a gravitational field, $p = p_0 + \rho g z$, where p_0 is the constant ambient pressure, and $\vec{g} = -g\hat{z}$ is the gravitational acceleration. The normal stress balance thus requires that the interface satisfy the *Young-Laplace Equation*:

$$\rho g z \;=\; \sigma \, \nabla \cdot \mathbf{n} \quad . \tag{4}$$

The vertical gradient in fluid pressure must be balanced by the curvature pressure; as the gradient is constant, the curvature must likewise increase linearly with z. Such a situation arises in the static meniscus (see Figure 1).

The shape of the meniscus is prescribed by two factors: the contact angle between the air-water interface and the log, and the balance between hydrostatic pressure and curvature pressure. We

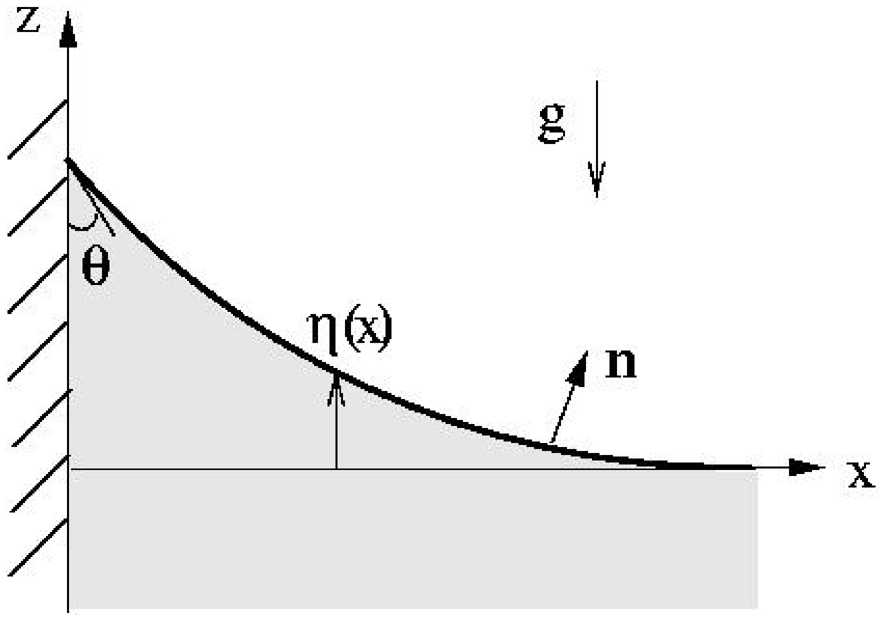

Figure 1: A definitional sketch of a planar meniscus at an air-water interface. The free surface is defined by $z = \eta(x)$, varying from its maximum elevation at its point of contact with the wall ($x = 0$) to zero at large x. The shape is prescribed by the Young-Laplace equation.

treat the contact angle, θ, as given; it depends on the physics of the log-water-air interaction. The normal force balance is expressed by the Young-Laplace equation, where now $\rho = \rho_w - \rho_a \approx \rho_w$ is the density difference between water and air.

We define the free surface by $z = \eta(x)$; equivalently, we define a functional $f(x, z) = z - \eta(x)$ that vanishes on the surface. The normal to the surface is thus

$$\mathbf{n} \;=\; \frac{\nabla f}{|\nabla f|} \;=\; \frac{\hat{z} - \eta'(x)\mathbf{x}}{(1 + \eta'(x)^2)^{1/2}} \tag{5}$$

As deduced in Appendix A, the curvature of the free surface, $\nabla \cdot \hat{n}$, may be expressed as

$$\nabla \cdot \hat{n} = \frac{\eta_{xx}}{(1 + \eta_x^2)^{3/2}} \approx \eta_{xx}. \tag{6}$$

Assuming that the slope of the meniscus remains small, $\eta_x << 1$, allows one to linearize equation (13), so that (11) assumes the form:

$$\rho g \eta \;=\; \sigma \eta_{xx} \quad . \tag{7}$$

Applying the boundary condition $\eta(\infty) = 0$ and the contact condition $\eta_x(0) = -\cot\theta$, and solving (16) thus yields:

$$\eta(x) = \ell_c \cot(\theta) e^{-x/\ell_c}, \tag{8}$$

where $\ell_c = \sqrt{\frac{\sigma}{\rho g}}$ is the capillary length. The meniscus formed by a log in water is exponential, dying off on the scale of ℓ_c.

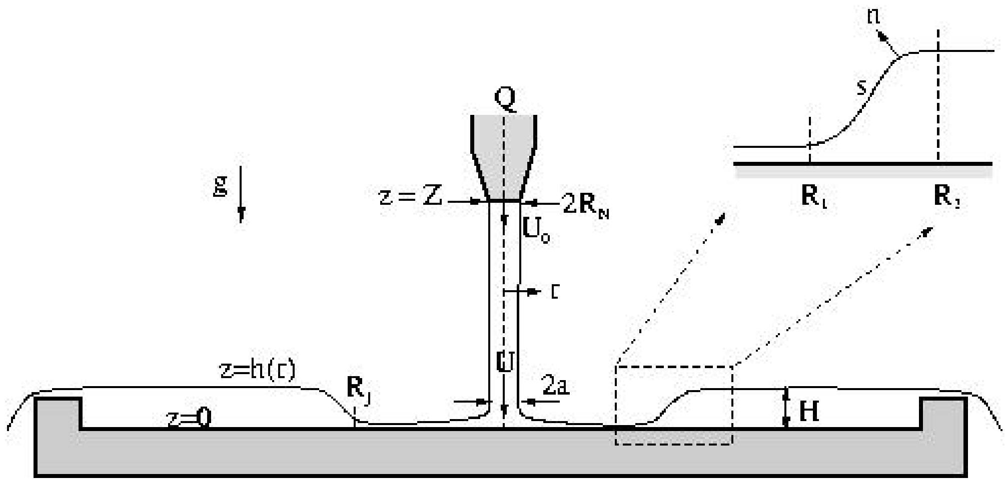

Figure 2: A schematic illustration of the geometry of the circular hydraulic jump. A jet of radius a impacts a reservoir of outer depth H at a speed U. The curvature force associated with the surface tension σ depends only on the geometry of the jump; specifically, on the radial distance $\Delta R = R_2 - R_1$ and arclength s between the two nearest points up and downstream of the jump at which the surface $z = h(r)$ has vanishing slope.

3.3 Radial force on a circular hydraulic jump

Hydraulic jumps may be generated when a vertical jet strikes a flat plate. The jet spreads radially, giving rise to a fluid layer that generally thins with radius until reaching a critical radius at which it increases dramatically (see Figure 2 and http://www-math.mit.edu/ bush/jump.htm). We here calculate the total radial force acting on the jump surface owing to the curvature of the jump between points A and B, located at radii R_1 and R_2, respectively. Assume that the points A and B are the points nearest the jump, respectively, upstream and downstream, at which the slope of the surface vanished identically.

We know that the curvature force per unit area is $\sigma(\nabla \cdot \mathbf{n})\mathbf{n}$. We must integrate the radial component of this force over the jump surface:

$$F_c \;=\; \sigma \int\!\!\int_S \nabla \cdot \mathbf{n}\; (\mathbf{n} \cdot \hat{\mathbf{r}})\; dS \tag{9}$$

Now defining the surface as $z = h(r)$ allows us to express the area element as

$$dS \;=\; r\; d\theta (dr^2 + dz^2)^{1/2} \;=\; r\; d\theta\; (1 + h_r)^{1/2}\; dr\;, \tag{10}$$

so that our radial force assumes the form

$$F_c \;=\; \sigma \int_0^{2\pi} \int_{R_1}^{R_2} \nabla \cdot \mathbf{n}\; (\mathbf{n} \cdot \hat{\mathbf{r}})\; r\; (1 + h_r)^{1/2}\; dr\; d\theta\;. \tag{11}$$

Now we use the appropriate forms for $\mathbf{n}$ and $\nabla \cdot \mathbf{n}$ from Appendix A, equation (41):

$$\mathbf{n} \;=\; \frac{\hat{z} - h_r \hat{r}}{(1 + h_r^2)^{1/2}} \quad , \quad \nabla \cdot \mathbf{n} \;=\; -\frac{1}{r}\frac{d}{dr}\,\frac{r h_r}{(1 + h_r^2)^{1/2}} \quad , \tag{12}$$

so that

$$(\nabla \cdot \mathbf{n})(\mathbf{n} \cdot \hat{\mathbf{r}}) \;=\; \frac{h_r}{(1+h_r^2)^{1/2}} \; \frac{1}{r}\frac{d}{dr} \; \frac{r h_r}{(1+h_r^2)^{1/2}} \tag{13}$$

and the radial curvature force becomes

$$F_c \;=\; 2\pi\sigma \int_{R_1}^{R_2} \frac{h_r}{(1+h_r^2)^{1/2}} \; \frac{1}{r}\frac{d}{dr} \left(\frac{r h_r}{(1+h_r^2)^{1/2}} \right) \; r\;(1+h_r)^{1/2}\; dr \tag{14}$$

$$\;=\; 2\pi\sigma \int_{R_1}^{R_2} \; h_r \; \frac{d}{dr} \left(\frac{r h_r}{(1+h_r^2)^{1/2}} \right) \; dr \tag{15}$$

Integrating by parts, $\int_a^b \; udv \;=\; uv|_a^b \;-\; \int_a^b \; v \; du$ with $u = h_r$, $v = \frac{r h_r}{(1+h_r^2)^{1/2}}$, yields

$$F_c \;=\; 2\pi\sigma \; \left[\; r h_r^2 \frac{1}{(1+h_r^2)^{1/2}}|_{R_1}^{R_2} \;-\; \int_{R_1}^{R_2} \frac{r h_r h_r r}{(1+h_r^2)^{1/2}} \; dr \; \right] \tag{16}$$

$$= -2\pi\sigma \; \int_{R_1}^{R_2} \; \frac{r h_r h_r r}{(1+h_r^2)^{1/2}} \; dr \tag{17}$$

Integrating by parts again, with $u = r$, $v = (1+h_r^2)^{1/2}$, yields

$$F_c \;=\; 2\pi\sigma \; \left[\; r(1+h_r^2)^{1/2}|_{R_1}^{R_2} \;-\; \int_{R_1}^{R_2} (1+h_r^2)^{1/2} dr \; \right] \tag{18}$$

$$= \; -\,2\pi\sigma \left[(R_2 - R_1) \;-\; \int_{R_1}^{R_2} (1+h_r^2)^{1/2} \; dr \; \right] \tag{19}$$

since $h_r = 0$ at $r = R_1, R_2$ by assumption. We note also that

$$\int_{R_1}^{R_2} (1+h_r^2)^{1/2} \; dr \;=\; \int_A^B (dr^2 + dz^2)^{1/2} \;=\; \int_A^B d\ell \;=\; S \;, \tag{20}$$

where S is defined as the total arclength of the surface between points A and B. We define $\Delta R = R_1 - R_2$ in order to obtain the simple result:

$$F_c \;=\; 2\pi\sigma(S - \Delta R) \quad . \tag{21}$$

We note that this relation yields reasonable results in two limits of interest. First, for a flat interface, $S = \Delta R$, so that $F_c = 0$. Second, for an abrupt jump in height of ΔH, $\Delta R = 0$ and $S = \Delta H$, so that $F_c = 2\pi\sigma\Delta H$. This result is commensurate with the total force exerted by a cylindrical annulus of radius R and height ΔH, which is deduced from the product of σ, the area $2\pi R \Delta H$ and the curvature $1/R$:

$$F_c \;=\; \sigma \; (2\pi R \Delta H \; \frac{1}{R}) \;=\; 2\pi\sigma\Delta H \tag{22}$$

The influence of this force was found to be significant for small hydraulic jumps. Its importance relative to the hydrostatic pressure in containing the jump is given by

$$\frac{\text{Curvature}}{\text{Gravity}} \;=\; \frac{\sigma/R}{\rho g \Delta H} \;=\; \frac{H}{R} B_0^{-1} \tag{23}$$

where the Bond number is defined here as

$$B_0 \;=\; \frac{\rho g H^2}{\sigma} \quad . \tag{24}$$

The simple result (19) was derived by Bush & Aristoff (2003), who also presented the results of an experimental study of circular hydraulic jumps. Their experiments indicated that the curvature force becomes appreciable for jumps with characteristic radius of less than 3 cm.

While the influence of surface tension on the radius of the circular hydraulic jump is generally small, it may have a qualitative influence on the shape of the jump. In particular, it may prompt the axisymmetry-breaking instability responsible for the polygonal hydraulic jump structures discovered by Elegaard *et al.* (*Nature*, 1998), and more recently examined by Bush, Hosoi & Aristoff (2004). See http://www-math.mit.edu/ bush/jump.htm.

3.4 Floating Bodies

Floating bodies must be supported by some combination of buoyancy and curvature forces. Specifically, since the fluid pressure beneath the interface is related to the atmospheric pressure P_0 above the interface by

$$p \;=\; P_0 \;+\; \rho g z \;+\; \sigma \nabla \cdot \mathbf{n} \quad ,$$

one may express the vertical force balance as

$$Mg \;=\; \mathbf{z} \cdot \int_c -p \,\mathbf{n}\, d\ell \;=\; F_b \;+\; F_c \quad . \tag{25}$$

The buoyancy force

$$F_b \;=\; \mathbf{z} \cdot \int_C \rho g z \,\mathbf{n}\, d\ell \;=\; \rho g V_b \tag{26}$$

is thus sim

bove the object and inside the line of tangency (Figure 3). A simple expression for the curvature force may be deduced using the first of the Frenet-Serret equations (see Appendix B).

$$F_c \;=\; \mathbf{z} \cdot \int_C \sigma(\nabla \cdot \mathbf{n})\mathbf{n}\, d\ell \;=\; \sigma \mathbf{z} \cdot \int_C \frac{d\mathbf{t}}{d\ell}\, d\ell \;=\; \sigma \mathbf{z} \cdot (\mathbf{t_1} - \mathbf{t_2}) \;=\; 2\sigma \sin\theta \tag{27}$$

At the interface, the buoyancy and curvature forces must balance precisely, so the Young-Laplace relation is satisfied:

$$0 \;=\; \rho g z \;+\; \sigma \nabla \cdot \mathbf{n} \tag{28}$$

Integrating the fluid pressure over the meniscus yields the vertical force balance:

$$F_b^m \;+\; F_c^m \;=\; 0 \quad . \tag{29}$$

where

$$F_b^m \;=\; \mathbf{z} \cdot \int_{C_m} \rho g z \mathbf{n}\, d\ell \;=\; \rho g V_m \tag{30}$$

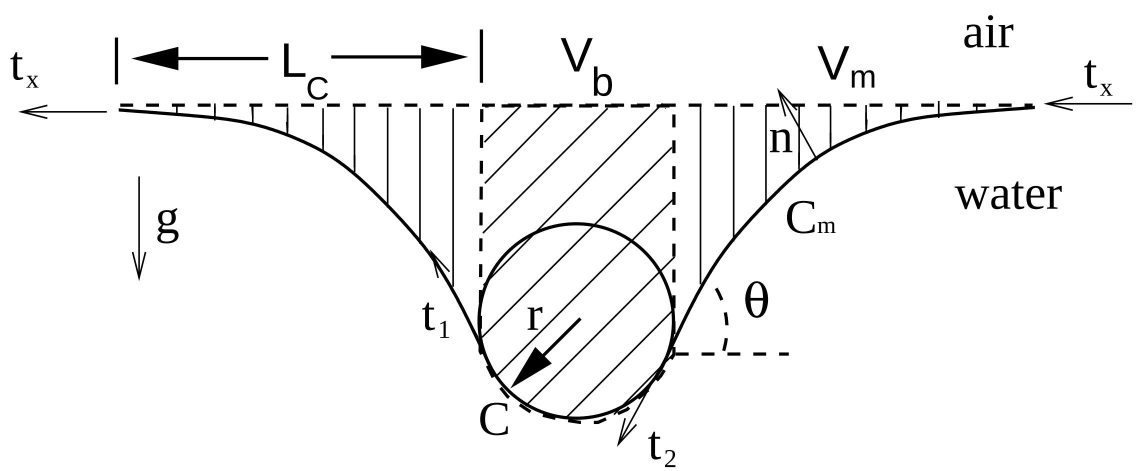

Figure 3: A non-wetting two-dimensional body of radius r and mass M floats on a free surface with surface tension σ. In general, its weight Mg must be supported by some combination of curvature and buoyancy forces. V_b and V_m denote the fluid volumes displaced, respectively, inside and outside the line of tangency.

$$F_c^m \;=\; \mathbf{z}\cdot\int_{C_m}\sigma(\nabla\cdot\mathbf{n})\mathbf{n}\;d\ell \;=\; \sigma\mathbf{z}\cdot\int_{C_m}\frac{d\mathbf{t}}{d\ell}\;d\ell \;=\; \sigma\mathbf{z}\cdot(\mathbf{t_x}-\mathbf{t_2}) \;=\; -\,2\sigma\,\sin\theta \tag{31}$$

where we have again used the Frenet-Serret equations to evaluate the curvature force.

Equations (27)-(31) thus indicate that the curvature force acting on the floating body is expressible in terms of the fluid volume displaced *outside* the line of tangency:

$$F_c \;=\; \rho g V_m \quad . \tag{32}$$

The relative magnitude of the buoyancy and curvature forces supporting a floating, non-wetting body is thus prescribed by the relative magnitudes of the volumes of the fluid displaced inside and outside the line of tangency:

$$\frac{F_b}{F_c} \;=\; \frac{V_b}{V_m} \quad . \tag{33}$$

For 2D bodies, we note that since the meniscus will have a length comparable to the capillary length, $\ell_c = (\sigma/(\rho g))^{1/2}$, the relative magnitudes of the buoyancy and curvature forces,

$$\frac{F_b}{F_c} \;\approx\; \frac{r}{\ell_c} \quad , \tag{34}$$

is prescribed by the relative magnitudes of the body size and capillary length. Very small floating objects ($r \ll \ell_c$) are supported principally by curvature rather than buoyancy forces. This result has been extended to three-dimensional floating objects by Keller (1998, *Phys. Fluids*, **10**, 3009-3010).

Water-walking Insects

Figure 4: Water-walking insects deflect the free surface, thus generating curvature forces that bear their weight. The water strider has characteristic length 1cm and weight 1-10 mg. See http://www-math.mit.edu/ dhu/Striderweb/striderweb.html .

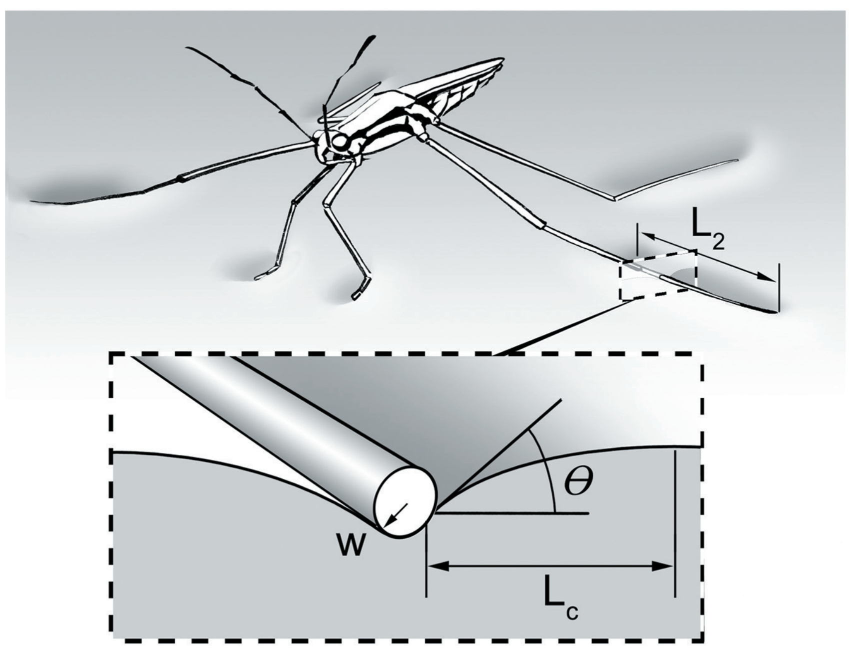

Figure 5: The water strider legs are covered with hair, rendering them effectively non-wetting. The tarsal segment of its legs rest on the free surface. The free surface makes an angle θ with the horizontal, resulting in an upward curvature force per unit length $2\sigma\sin\theta$ that bears the insect's weight.

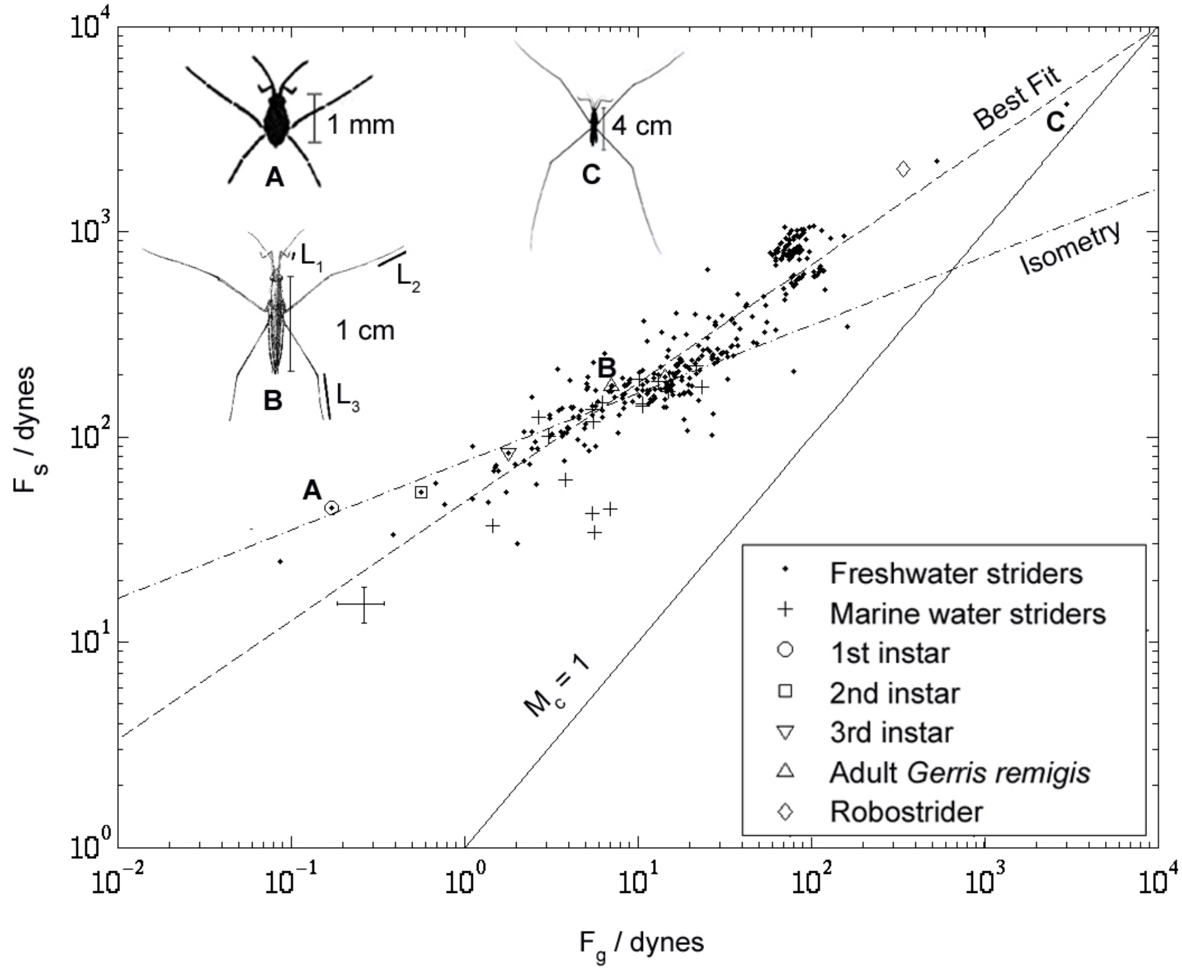

Figure 6: The relation between the maximum curvature force $F_s = \sigma P$ and body weight $F_g = Mg$ for 342 species of water striders. $P = 2(L_1 + L_2 + L_3)$ is the combined lengths of the tarsal segments (see strider B). From Hu, Chan & Bush (*Nature*, **424**, 2003).

Small objects such as paper clips, pins or insects may reside at rest on a free surface provided the curvature force induced by their deflection of the free surface is sufficient to bear their weight. For example, for a body of contact length L and total mass M, static equilibrium on the free surface requires that:

$$\frac{Mg}{2\sigma L \sin\theta} < 1 \qquad (35)$$

where θ is the angle of tangency of the floating body.

This simple criterion is an important geometric constraint on water-walking insects. Figure 6 indicates the dependence of contact length on body weight for over 300 species of water-striders, the most common water walking insect. Note that the solid line corresponds to the requirement (35) for static equilibrium. Smaller insects maintain a considerable margin of safety, while the larger striders live close to the edge. The size of water-walking insects is limited by the constraint (35).

If body proportions were independent of size L, one would expect the body weight to scale as L^3 and the curvature force as L. Isometry would thus suggest a dependence of the form $F_c \sim F_g^{1/3}$, represented as the dashed line in Figure 6. The fact that the best fit line has a slope considerably larger than 1/3 indicates a variance from isometry: the legs of large water striders are proportionally longer.

Appendix A: Computing curvatures

We see the appearance of the divergence of the surface normal, $\nabla \cdot \mathbf{n}$, in the normal stress balance. We proceed by briefly reviewing how to formulate this curvature term in two common geometries.

In cartesian coordinates (x, y, z), we consider a surface defined by $z = h(x, y)$. We define a functional $f(x, y, z) = z - h(x, y)$ that necessarily vanishes on the surface. The normal to the surface is defined by

$$\mathbf{n} = \frac{\nabla f}{|\nabla f|} = \frac{\hat{z} - h_x \hat{x} - h_y \hat{y}}{(1 + h_x^2 + h_y^2)^{1/2}} \tag{36}$$

and the local curvature may thus be computed:

$$\nabla \cdot \mathbf{n} = \frac{-(h_{xx} + h_{yy}) - (h_{xx} h_y^2 + h_{yy} h_x^2) + 2 h_x h_y h_{xy}}{(1 + h_x^2 + h_y^2)^{3/2}} \tag{37}$$

In the simple case of a two-dimensional interface, $z = h(x)$, these results assume the simple forms:

$$\mathbf{n} = \frac{\hat{z} - h_x \hat{x}}{(1 + h_x^2)^{1/2}} \quad , \quad \nabla \cdot \mathbf{n} = \frac{-h_{xx}}{(1 + h_x^2)^{3/2}} \quad . \tag{38}$$

Note that $\mathbf{n}$ is dimensionless, while $\nabla \cdot \mathbf{n}$ has the units of $1/L$.

In 3D polar coordinates (r, θ, z), we consider a surface defined by $z = h(r, \theta)$. We define a functional $g(r, \theta, z) = z - h(r, \theta)$ that vanishes on the surface, and compute the normal:

$$\mathbf{n} = \frac{\nabla g}{|\nabla g|} = \frac{\hat{z} - h_r \hat{r} - \frac{1}{r} h_\theta \hat{\theta}}{(1 + h_r^2 + \frac{1}{r^2} h_\theta^2)^{1/2}} \quad , \tag{39}$$

from which the local curvature is computed:

$$\nabla \cdot \mathbf{n} = \frac{-h_{\theta\theta} - h_r^2 h_{\theta\theta} + h_r h_\theta - r h_r - \frac{2}{r} h_r h_\theta^2 - r^2 h_{rr} - h_{rr} h_\theta^2 + h_r h_\theta h_{r\theta}}{r^2 (1 + h_r^2 + \frac{1}{r^2} h_\theta^2)^{3/2}} \quad . \tag{40}$$

In the case of an axisymmetric interface, $z = h(r)$, these results reduce to:

$$\mathbf{n} = \frac{\hat{z} - h_r \hat{r}}{(1 + h_r^2)} \quad , \quad \nabla \cdot \mathbf{n} = \frac{-r h_r - r^2 h_{rr}}{r^2 (1 + h_r^2)^{3/2}} \quad . \tag{41}$$

Appendix B: Frenet-Serret Equations

Differential geometry yields relations that are often useful in computing curvature forces on 2D interfaces.

$$(\nabla \cdot \mathbf{n})\ \mathbf{n} = \frac{d\mathbf{t}}{d\ell} \tag{42}$$

$$-(\nabla \cdot \mathbf{n})\ \mathbf{t} = \frac{d\mathbf{n}}{d\ell} \tag{43}$$

Note that the LHS of the first of (42) is proportional to the curvature pressure acting on an interface.